Pacific Northwest NATIONAL LABORATORY

MRP Microreactor Program

PNNL-39896

Shock and Vibration Assessment for Microreactor Transportation

September 2026

Jeriah A. Whitley
Connor J. Mack
Dina E. Carpenter-Graffy
Steven J. Maheras

U.S. DEPARTMENT of ENERGY

Prepared for the U.S. Department of Energy
under Contract DE-AC05-76RL01830

DISCLAIMER

This report was prepared as an account of work sponsored by an agency of the United States Government. Neither the United States Government nor any agency thereof, nor Battelle Memorial Institute, nor any of their employees, makes **any warranty, express or implied, or assumes any legal liability or responsibility for the accuracy, completeness, or usefulness of any information, apparatus, product, or process disclosed, or represents that its use would not infringe privately owned rights**. Reference herein to any specific commercial product, process, or service by trade name, trademark, manufacturer, or otherwise does not necessarily constitute or imply its endorsement, recommendation, or favoring by the United States Government or any agency thereof, or Battelle Memorial Institute. The views and opinions of authors expressed herein do not necessarily state or reflect those of the United States Government or any agency thereof.

PACIFIC NORTHWEST NATIONAL LABORATORY
operated by
BATTELLE
for the
UNITED STATES DEPARTMENT OF ENERGY
under Contract DE-AC05-76RL01830

Printed in the United States of America

Available to DOE and DOE contractors from
the Office of Scientific and Technical Information,
P.O. Box 62, Oak Ridge, TN 37831-0062
www.osti.gov
ph: (865) 576-8401
fax: (865) 576-5728
email: reports@osti.gov

Available to the public from the National Technical Information Service
5301 Shawnee Rd., Alexandria, VA 22312
ph: (800) 553-NTIS (6847)
or (703) 605-6000
email: info@ntis.gov
Online ordering: http://www.ntis.gov

PNNL-39896

Shock and Vibration Assessment for Microreactor Transportation

September 2026

Jeriah A. Whitley
Connor J. Mack
Dina E. Carpenter-Graffy
Steven J. Maheras

Prepared for
the U.S. Department of Energy
under Contract DE-AC05-76RL01830

Pacific Northwest National Laboratory
Richland, Washington 99354

Abstract

This report assesses the potential shock and vibration effects experienced by microreactors during road transportation. Because transportation conditions may vary with reactor design and whether fuel or radioactive materials are shipped concurrently, the study reviews applicable federal and state regulations, standards, and experimental considerations. A literature review of heavy-duty truck transportation and nuclear fuel cask transport was used to identify relevant factors influencing possible vibration and shock effects, including road quality, vehicle speed, suspension characteristics, payload stiffness, and reactor placement in the transport vehicle. The review indicates that these variables can affect both the magnitude and frequency of the loads transmitted to the reactor and its supporting systems. To support future testing, a transportation route selection algorithm was developed to identify candidate routes based on road quality, using the International Roughness Index (IRI) as a key metric. Selection of a route with the lowest IRI would provide a baseline for correlating road conditions with measured shock and vibration responses. The report also outlines sensor performance requirements, environmental measurements, material integrity assessments, and functional requirements needed to evaluate transportation impacts and inform the design of future microreactor transport experiments.

The objective of this report is to provide a high-level introduction into the shock and vibration associated with microreactor transport. A companion document, *MARVEL Shock and Vibration Test Plan* (Peoples et al. 2026) establishes the procedures, functional objectives, and laboratory testing methodology for transportation shock and vibration qualification, building directly upon the functions and requirements developed in the *MARVEL Reactor Shock and Vibration Functions and Requirements Document* (Stewart et al. 2026).

Acknowledgments

Pacific Northwest National Laboratory is operated by Battelle Memorial Institute for the Department of Energy (DOE). This work was prepared for the DOE, Office of Nuclear Energy, and sponsored by the DOE Microreactor Program.

This manuscript was edited using GPT-4o (OpenAI) for grammar and clarity. All content was drafted by the authors and finalized with AI assistance.

Acronyms and Abbreviations

ADS	Accelerator-Driven Subcritical Reactor
ASME	American Society of Mechanical Engineers
CFR	Code of Federal Regulations
DC	Direct Current
DOD/DOW	United States Department of Defense/Department of War
DOE	Department of Energy
DOT	Department of Transportation
FHWA	Federal Highway Administration, U.S. Department of Transportation
HALEU	High-assay Low-Enriched Uranium
HALEU-UF6	High-assay Low-Enriched Uranium Hexafluoride
HPMS	Highway Performance Monitoring System
HTGR	High-Temperature Gas-Cooled Reactor
Hz	Hertz
INL	Idaho National Laboratory
IRI	International Roughness Index
LEU	Low-Enriched Uranium
LEU+	Low-Enriched Uranium Plus
LFR	Lead-Cooled Fast Reactor
LWR	Light Water Reactor
MARVEL	Microreactor Applications Research Validation and Evaluation
MEMS	Micro-Electro Mechanical System
MSR	Molten Salt Reactor
MW	Megawatt
MWe	Megawatts of Electrical Power
MWth	Megawatts of Thermal Power
NRC	National Regulatory Commission
ODE	Ordinary Differential Equation
PSD	Power Spectral Density
PSR	Present Serviceability Rating
PWR	Pressurized Water Reactor
SFR	Sodium-Cooled Fast Reactor
SMR	Small Modular Nuclear Reactor
START	Stakeholder Tool for Assessing Radioactive Transport
TRISO	Tri-structural Isotropic Fuel
U.S.	United States of America
YH	Yttrium Hydride

Contents

Abstract ii
Acknowledgments iii
Acronyms and Abbreviations iv
1.0 Microreactors Background 1
2.0 Regulations and Standards for Microreactor Transportation 9
2.1 State Regulations and Policies 11
3.0 Shock and Vibration Physics Background 12
4.0 Relevant Transportation Literature Background 13
4.1 Road Quality and Vibration Energy 13
4.2 Vehicle Speed 13
4.3 Vehicle Suspension Type 14
4.4 Payload and System Dynamics 14
4.4.1 Payload Stiffness 15
4.4.2 Payload Position and Axes of Acceleration 15
4.4.3 Ranges of Frequency Response 16
4.4.4 Extreme Shock Events 17
5.0 Shock and Vibration Analysis 18
5.1 Transportation Route Considerations 18
5.1.1 Road Roughness 18
5.1.2 START Route Optimization 20
5.2 Accelerometers and Other Sensors 23
5.3 Microreactor Integrity Assessment 24
5.3.1 Considerations for Metallic Reactor Components 25
5.3.2 Considerations for Ceramic Reactor Components 25
5.4 Functions and Requirements for Shock and Vibration Testing 26
6.0 Conclusion 28
7.0 References 29

Figures

Figure 1. Diagram of the quarter-car model, showing IRI as a function of the surface evaluation (y, measured by in-situ road surveys) and the mass displacement (Z_s, Z_u) of a dual-spring system (with spring constants k_t, k_s) (Lin et al. 2022). 19

Figure 2. Distribution of IRI for the national highway network across the U.S. and individual states (FHWA 2026). 20

Figure 3. Representative results of a route optimization study for road transport between the Port of Seattle to INL. 21

Figure 4. Resulting metrics from the developed transportation route selection algorithm, which utilize publicly available HPMS road quality data. 22

Tables

Table 1. Current microreactor vendors 4

Table 2. The summary points within the subsections of 10 CFR, Part 71, which provides guidance related to fueled microreactor transport. 10

Table 3. The summary points within the subsections of 10 CFR Part 73, Subpart E. 11

Table 4. List of different types of accelerometers that could be used for future shock and vibration experiments. 24

Table 5. Functions and requirements for shock and vibration testing for MARVEL reactor shock and vibration study. 26

1.0 Microreactors Background

Nuclear-generated power is not a nascent technology; the first nuclear reactor designed to produce electricity was the Experimental Breeder reactor in 1951 (World Nuclear Association 2026a). However, as nuclear technology advances beyond the stationary infrastructure of conventional nuclear power plants, the design characteristics of transportable microreactor systems will play an increasingly important role in determining the feasibility, requirements, and safety considerations of transport in the United States (U.S.). For this reason, the following section will highlight some of the operational differences of advanced nuclear technology.

The general principle of operation of a nuclear generator is based on nuclear fission. A radioactive fuel, typically enriched uranium containing a higher concentration of the U-235 isotope, undergoes fission when the nuclei of its atoms are split. This process releases a tremendous amount of heat, which is used to heat water to produce steam. The high-pressure steam drives large turbines, converting thermal energy into mechanical energy. The mechanical energy is then converted by an electrical generator into usable electrical energy (World Nuclear Association 2026a).

In the last few decades, advanced nuclear technology (often referred to as Generation III+ and IV) has progressed to include reactors that have key differences from conventional nuclear reactor design. For a conventional nuclear power plant, a rough estimate of capacity would be around 1,000 megawatts (MW) of electrical power (MWe) generation (Derr 2022). For advanced nuclear systems, the upper end of a small modular nuclear reactor (SMR) can be around 300 MWe, and microreactors can have capacities up to 50 MWe, though many designs can operate with electrical outputs closer to 20 MWe (NUSCALE n.d.).

Advanced reactors can also utilize different fuels and coolants compared to historical nuclear power plants. While some advanced reactor designs still utilize the most common form of nuclear fuel, a low-enriched uranium (LEU) fuel that has an isotropic concentration of U-235 < 5%, some advanced reactors can use high-assay low-enriched uranium fuel (HALEU), which has concentrations of 5% < U-235 < 20% (Tarakanov 2023). HALEU hexafluoride (HALEU-UF6) can be processed and converted in different ways to a provide a variety of fuel forms, including uranium dioxide ceramic oxide pellets, uranium fuel dispersed in a molten salt, metallic uranium alloy, or into tri-structural isotropic fuel (TRISO), which consists of spherical kernels made of either uranium dioxide or uranium oxycarbide and coated in multiple carbon and silicon carbide-based layers (Nuclear Engineering International 2024).

Two key motivations that led to the growing field of SMR or microreactor research include passive safety systems and transportability. Compared to conventional nuclear power plants, advanced reactors have been designed so that passive, physics-based processes govern safety-crucial systems—such as heat removal via air circulation, convection, gravity, and self-pressurization (CNSC n.d.)—without human intervention. This is advantageous because there would be fewer staffing needs, and the passive safety controls can help to mitigate operator error, which has led to historical nuclear accidents in the past.

Additionally, the compact size and modular design of microreactors could enable them to be pre-fabricated and transported to deployment sites. Unlike conventional nuclear power plants, which require years of infrastructure development and construction, microreactors could be deployed much faster to deliver energy to locations urgently needing assistance. This capability could be especially valuable to areas affected by natural disasters or grid outages. In addition, microreactors could provide resilience to energy-intensive facilities such as military installations

and industrial plants. Depending on the design, microreactors could be deployed individually or combined into modular systems to provide varying levels of power generation based on the energy requirements of the deployment site. Microreactors can also either be connected to the grid to sell back power to the utility or be islanded as part of a microgrid and serve as back-up power to maintain continuity of operations in the case of a grid-outage or peak-energy cost time (Office of Nuclear Energy n.d.).

The transportability of SMRs or microreactors is one of the key advantages compared to conventional reactors. However, the fuel type, whether fuel is transported with the reactor, and the reactor type will all be important factors when determining transport logistics; different reactors and their respective systems could mean different vulnerabilities during transport. A variety of advanced nuclear reactor designs are currently under development. The following section provides a brief overview of highest technology readiness level microreactor (water-cooled reactors), as well as key advanced reactor systems, and highlights examples of reactor developers working to advance these technologies. **Table 1** contains a list of current microreactor vendors.

- **Water-cooled reactor**: Includes both light water reactors (LWRs) or heavy water reactors. The three most common reactor designs are pressurized water reactors (PWRs), boiling water reactors, or pressurized heavy water reactors (World Nuclear Association n.d.). An example is the Last Energy, Inc., PWR-20 PWR reactor, which has an electrical capacity of 20 MWe and uses LEU fuel and water as coolant (Last Energy n.d.).
- **Liquid metal-cooled fast reactor:** Generation IV fast reactors utilize a fast neutron spectrum in which neutrons produced by fission are not intentionally slowed down by a moderator, maintaining their high-kinetic energy (Nuclear Engineering International 2024; World Nuclear Association 2026b). Reactors that utilize liquid metal coolants can operate at much higher temperatures, depending on the reactor design and coolant type. Higher operating temperatures can produce higher thermal conversion efficiencies. For sodium-cooled fast reactors (SFRs), approximate outlet temperatures could range from 500–550 degrees Celsius, with a possible range in capacity of 50–150 MWe. Alternatively, for lead-cooled fast reactors (LFRs), outlet temperatures could reach around 480–570 degrees Celsius, with 20–180 MWe possible capacity (GenIV n.d.).
- **Molten salt reactor (MSR):** MSRs utilize molten salt (commonly fluoride and chloride salts) as the coolant and the reactor core exists in a liquid state. Fuels for this type of reactor can vary. These reactors could have a thermal neutron spectrum—where the kinetic energy of the neutrons has been lowered to reach equilibrium with the surrounding environment via a moderator—or a fast neutron spectrum (World Nuclear Association 2025). Salts can be reactive when exposed to water or air, so this type of reactor would require special considerations to avoid contamination during transport with fuel and during operation. An example design has been proposed by Alpha Tech, the Micro Molten Salt Reactor (ARC Generator), which utilizes fluoride salt as a coolant, yttrium hydride (YH) as the moderator material, and LEU fuel (Alpha Tech n.d.). The estimated capacity is 12 MWe.
- **High-temperature reactors:** All high-temperature reactors use TRISO particle fuel; however, the designs often vary depending on the coolant type (Nuclear Engineering International 2024). The two most common Generation IV high-temperature reactor designs are high-temperature gas-cooled reactors (HTGR) and high-temperature, salt-cooled

reactors.[1] An example of an HTGR is the Holos-Quad reactor developed by HolosGen LLC (HolosGen n.d.), which utilizes helium and carbon dioxide gases as coolants, a graphite moderator, and TRISO fuel (Stauff et al. 2022). This single transportable reactor has an approximate capacity of 3–13 MWe.

For the purposes of this study, the primary focus will be on smaller-sized microreactors with an electrical generation capacity around 5–50 MWe.

The advantage of microreactors being modular and transportable also remains a key challenge in the deployment of this technology. Many unknowns remain regarding the impact of shock and vibration on the microreactors during transit. The current federal and regional regulations for nuclear material transport are being evaluated to ensure there are no gaps for future transport of fueled or non-fueled reactors. Other key considerations for microreactor transport include route selection and the necessary verification steps to ensure no significant damage will occur during transport, which could impact microreactor operation in the future. This document highlights key considerations for the transportation of microreactors, presents a shock and vibration assessment of the primary factors relevant to transport, and outlines a future research plan for collecting and analyzing data to support transportation assessments.

It should be noted that there are other factors relevant in the planning process for the transport of microreactors; however, they fall outside of the scope of this analysis. If a microreactor is shipped with nuclear fuel, appropriate safeguard protocols would be required to prevent any loss, theft, or other adverse events involving the nuclear material. It would also be salient to determine the necessary agencies, emergency response teams, and emergency response training needed for any transport event to mitigate potential harm to the environment and human personnel. Finally, early involvement and engagement with the community and stakeholders along potential transportation routes should be considered to address concerns, facilitate coordination, and reduce the potential for project delays.

[1] Salts can be reactive when exposed to water or air, so the salt-cooled version of this reactor would require special considerations to avoid contamination during transport with fuel, as well as during operation.

Table 1. Current microreactor vendors.

Developer	Design Name	Reactor Type	Power Output (MWe/MWth)	Enrichment	Fuel Form	Coolant	Moderator	Refueling Interval	Transportability	Conversion Technology
Aalo Atomics	Aalo-1; Aalo-X (test reactor)	SFR	10 MWe/ 30 MWth	LEU	UO2	Sodium	Graphite	3–5 years	Movable	Steam turbine
Alpha Tech Research	ARC Generator	MSR	12 MWe/ 30 MWth	LEU	Uranium-bearing fluoride fuel salt	Fluoride salt	YH	N/A (continuous fuel management)	Movable	Not publicly disclosed
Ampera	AMPERA subcritical thorium microreactor platform	ADS	15–30 MWe	Thorium	TRISO	Not publicly disclosed	Not publicly disclosed	30 years/ no planned refueling	Movable	Gas turbine
Antares Nuclear, Inc.	R1; Mark-0 (test reactor)	Heat pipe	0.1–1 MWe (R1 product range)	HALEU	TRISO	Sodium heat pipes	Graphite	4–6 years	Mobile	Gas turbine
Apollo Atomics, Inc.	Apollo compact PWR (commercial name not publicly disclosed)	LWR	1 MW demonstrator; 10 MW commercial pilot (basis not publicly specified)	LEU	Commercial-grade uranium fuel (form not publicly disclosed)	Water	Water	Not publicly disclosed	Movable	Steam turbine
Atlas Atomics	Advanced heavy-water reactor (name not publicly disclosed)	Heavy water reactor	Not publicly disclosed	Not publicly disclosed	Not publicly disclosed	Not publicly disclosed	Heavy water	Not publicly disclosed	Not publicly disclosed	Not publicly disclosed
BWX Technologies	BANR (Project Pele related demonstration program)	HTGR	BANR: 50 MWth (electric output not publicly disclosed); Project Pele: 1.5 MWe	HALEU	TRISO	Helium	Graphite	5 years (BANR target)	Movable	Gas turbine

Developer	Design Name	Reactor Type	Power Output (MWe/MWth)	Enrichment	Fuel Form	Coolant	Moderator	Refueling Interval	Transportability	Conversion Technology
Deep Fission, Inc.	Gravity/ DFBR-1	LWR	Up to 15 MWe/ 45 MWth	LEU	Commercial PWR-type UO2 fuel assemblies	Water	Water	4–6 years	Stationary	Steam turbine
Deployable Energy	Unity Nuclear Battery	HTGR	1 MWe	LEU	UO2	Helium	Water	5 years	Movable	Not publicly disclosed
EE Capital LLC	ELYON-5	Heat pipe	5 MWe/ 16.7 MWth	HALEU	TRISO	Sodium heat pipes	Not publicly disclosed	10 years	Movable	Not publicly disclosed
Emerald Horizon	ADES	ADS	10 MWe/ 25 MWth (current public specification)	Thorium	ThF4-bearing fuel system	Molten salt	Not publicly disclosed	20 years	Movable	Not publicly disclosed
Forge Atomics	Ember	LWR	25 MWe	LEU	UO2 (PWR-derived)	Water	Water	Not publicly disclosed	Movable	Steam turbine
General Atomics	GA-TES	Liquid metal reactor	5 MWe baseline; scalable to 20 MWe	Not publicly disclosed	Uranium-zirconium-hydride	Liquid metal	Hydrogen-bearing fuel matrix	Not publicly disclosed	Mobile	Steam turbine
Hadron Energy, Inc.	Halo MMR	LWR	10 MWe/ 35 MWth (lead configuration)	LEU+	Not publicly disclosed	Water	Water	10 years	Movable	Steam turbine
HolosGen LLC	Holos-Quad	HTGR	3–13 MWe (Holos-Quad configurations)	Not publicly disclosed	TRISO/ FCM-type fuel cartridges	Gas (company does not consistently specify one working fluid)	Graphite	~8–10 years	Mobile	Gas turbine
Kairos Power	ANPI microreactor offering (name not publicly disclosed)	HTGR	Not publicly disclosed	Not publicly disclosed	TRISO	Molten fluoride salt	Graphite	Not publicly disclosed	Not publicly disclosed	Not publicly disclosed
Last Energy, Inc.	PWR-20	LWR	20 MWe/ 80 MWth	LEU	UO2	Water	Water	6 years (company design basis)	Stationary	Steam turbine

Developer	Design Name	Reactor Type	Power Output (MWe/MWth)	Enrichment	Fuel Form	Coolant	Moderator	Refueling Interval	Transportability	Conversion Technology
Micro Nuclear, LLC	Microscale Nuclear Battery (MsNB)	MSR	5 MWe reference configuration	HALEU	UF4-bearing fuel salt	Molten fluoride salt	YH	~10 years	Movable	Gas turbine
NANO Nuclear Energy	KRONOS MMR; ZEUS; LOKI MMR	Multiple/ design-dependent	KRONOS: 45 MWth; LOKI: 10 kWe–3 MWe/ 1.5–5 MWth; ZEUS: not publicly disclosed	HALEU (design-specific details vary)	KRONOS/ LOKI: TRISO; ZEUS: sealed solid core	KRONOS/LOKI: Helium; ZEUS: no in-core fluid	Graphite (KRONOS/ LOKI)	Design-dependent; up to ~20 years claimed for some products	Movable	Multiple/ design-dependent
Natural Resources	MSR-1	MSR	Non-power research/ demonstration reactor (thermal rating not consistently disclosed in current public materials)	HALEU	Fuel dissolved in molten salt	Molten fuel salt	Graphite	N/A (research operations)	Stationary	Heat only/ none
Nuclear Energy USA	Morpheus Microreactor	LFR	3.5–50 MWe product range	HALEU	Not publicly disclosed	Lead	Graphite	5 years	Movable	Not publicly disclosed
NuCube Energy, Inc.	NuSun-1; NuSun-15; ART (research/test reactor)	Heat pipe	NuSun-1: ~1.3 MWe; NuSun-15: ~15 MWe	LEU+/ HALEU	TRISO	Heat pipes (working fluid not publicly standardized)	Graphite	Not publicly disclosed	Movable	Thermophotovoltaic
NuGen, LLC	NuGen Engine	HTGR	2–3 MWe	Not publicly disclosed	Not publicly disclosed	Gas	Not publicly disclosed	15 years	Mobile	Gas turbine
NuScale Power	NuScale Microreactor	Heat pipe	<10 MWe; 8–40 MWth concept range	HALEU	Metallic/ liquid uranium concept	Liquid metal/ heat pipes	Not publicly disclosed	~10 years	Movable	Thermophotovoltaic

Developer	Design Name	Reactor Type	Power Output (MWe/MWth)	Enrichment	Fuel Form	Coolant	Moderator	Refueling Interval	Transportability	Conversion Technology
Odin Electric, Inc.	Odin thorium-fueled generator (name not publicly disclosed)	Not publicly disclosed	10 kWe	Thorium	Not publicly disclosed	Not publicly disclosed	Not publicly disclosed	Not publicly disclosed	Not publicly disclosed	Not publicly disclosed
Oklo, Inc.	Aurora (15 MWe microreactor configuration)	SFR	15 MWe qualifying configuration (Aurora family extends above 50 MWe)	HALEU	U-Zr metal	Sodium	None (fast spectrum)	10–20 years (configuration-dependent)	Stationary	Not publicly disclosed
Radiant Industries	Kaleidos	HTGR	~1 MWe/ 3 MWth	HALEU	TRISO	Helium	Graphite	4–6 years	Mobile	Gas turbine
Scaled Atomics	MN-350	Not publicly disclosed	350 kWe/ ~1 MWth	Not publicly disclosed	Not publicly disclosed	Not publicly disclosed	Not publicly disclosed	10 years	Mobile	Gas turbine
Tam Fortis Solutions	Tam Fortis mobile microreactor (product name not publicly disclosed)	Heat pipe	40 kWe continuous	HALEU	TRISO	Liquid metal heat pipes	Not publicly disclosed	5 years	Mobile	Gas turbine
Terra Innovatum	SOLO	HTGR	1 MWe/ 5 MWth	LEU (4.95% U-235 baseline); higher enrichment options under evaluation	UO2 pellets in Zircaloy cladding	Helium	Solid moderator (not consistently identified in public summary)	Not publicly disclosed	Movable	Gas turbine
Valar Atomics	Ward 250	HTGR	250 kWth research reactor (public DOE design rating)	HALEU	TRISO	Helium	Graphite	Not publicly disclosed	Stationary	Thermoelectric
Vulcaris	VERMI	Heat pipe	~1 MWe	HALEU	Proprietary metallic fuel	Heat pipes	Not publicly disclosed	15+ years	Movable	Not publicly disclosed

Developer	Design Name	Reactor Type	Power Output (MWe/MWth)	Enrichment	Fuel Form	Coolant	Moderator	Refueling Interval	Transportability	Conversion Technology
Westinghouse	eVinci	Heat pipe	0.2–5 MWe/ ~13–15 MWth (configuration-dependent)	HALEU	TRISO	Sodium heat pipes	Solid moderator (company design)	8+ years	Movable	Not publicly disclosed
X-energy	XENITH	HTGR	3–10 MWe	HALEU	TRISO-X	Helium	Graphite	~3 years (current public design basis varies)	Movable	Gas turbine

Mobile = intended for routine relocation; Movable = transportable for deployment/retrieval but not routine relocation; Stationary = permanent installation.
ADS = accelerator-driven subcritical reactor, HALEU = High-assay low-enriched uranium (5–20% enriched), HTGR = high-temperature gas-cooled reactor, LEU = low-enriched uranium (< 5% enriched), LEU+ = low-enriched uranium plus (5–10% enriched), LFR = lead-cooled fast reactor, LWR = light water reactor, MSR = molten salt reactor, SFR = sodium-cooled fast reactor, TRISO = tri-structural isotropic nuclear fuel.

2.0 Regulations and Standards for Microreactor Transportation

There are many necessary procedures and requirements outlined by various regulatory bodies in the U.S. for shipping nuclear technology and fuels. While this report is focused on outlining the important considerations for a shock and vibration analysis, the following section highlights relevant regulations that can directly impact the feasibility, planning process, and implementation of microreactor transport efforts.

Two key variables that impact regulatory requirements are transportation mode and radioactive material. Several modes of transportation could be potentially used for microreactor transportation and warrant further investigation, including airplane, rail, maritime vessel, and heavy-duty truck transport. While this report will primarily focus on road transport, future research could provide useful information for the considerations and challenges associated with the other modes used for microreactor transportation.

The second factor impacting regulatory requirements is the fuel. Whether the reactor is transported in a fueled or unfueled state, whether the fuel is irradiated or not, the fuel form and the enrichment level will impact the applicable regulatory requirements for transportation.

The primary regulations governing the transport of hazardous materials (including radioactive materials) in the U.S. are established by the Department of Transportation (DOT) Pipeline and Hazardous Materials Safety Administration. Specifically, this would include the hazardous materials regulations contained in 49 Code of Federal Regulation (CFR) Parts 100 to 180. In addition, 49 CFR Part 385 contains requirements for hazardous materials permits, and 49 CFR Part 397 contains requirements for hazardous materials highway routing. Rail routing of hazardous materials is addressed in 49 CFR 172.820. These regulations apply to everyone shipping hazardous materials in commerce—including Department of Energy (DOE) and its contractors, as well as Department of Defense/Department of War (DOD/DOW) and its contractors.

DOE conducts shipments of radioactive materials according to its system of orders. The primary order for unclassified shipments is DOE Order 460.2C. DOD/DOW conducts shipments of hazardous materials according to the Defense Transportation Regulations (DTR) 4500.9-R, Chapter 204. Chapter 204 points to the DOT requirements in 49 CFR. An additional consideration would be that DOE and DOD/DOW may make hazardous materials shipments with a National Security Exemption (see 49 CFR 173.7[b]).

10 CFR Part 71 contains the Nuclear Regulatory Commission (NRC) regulations that govern the transport of radioactive material, including microreactors (10 CFR §§ 71.11–71.75). The key subparts are outlined in **Table 2** below.

Table 2. The summary points within the subsections of 10 CFR, Part 71, which provides guidance related to fueled microreactor transport.

10 CFR Part 71	*Overall Framework for Radioactive Material Packaging and Transportation*
§71.11	Specific exemptions from Part 71
§71.14	Exemptions for low-level material
§71.15	Exemption from fissile-material classification
§71.17	General license for use of NRC-approved packages
§71.22	General license for certain fissile material
§71.31–71.39	Package approval application and QA requirements
§71.41	Demonstration of compliance
§71.43	General package design requirements
§71.45	Lifting and tie-down
§71.47	Radiation limits
§71.51	Additional requirements for Type B packages
§71.55	Fissile material package requirements
§71.59	Arrays of fissile packages
§71.71	Normal conditions of transport
§71.73	Hypothetical accident conditions
§71.75	Special-form radioactive material qualification

The 10 CFR Part 71 proposed rulemaking, “Modernizing Package Certification Requirements,” was released July 27, 2026, and comments were due August 26, 2026 (91 FR 46869–46881, July 27, 2026). This proposed rulemaking revises 10 CFR 71.41 to allow use of NRC-endorsed methodology for transportation package approval and revises 10 CFR 71.47 to establish higher radiation dose rate limits (50 mrem/h–0.5 mSv/h) for some packages (e.g., microreactors) under exclusive use controls.

10 CFR Part 73 contains NRC security requirements for radioactive material shipments, including irradiated nuclear fuel (10 CFR §§ 73.24–73.38). These regulations would apply to commercial microreactor shipments (i.e., shipments not made for DOE or DOD/DOW) and are summarized in **Table 3** below.

Table 3. The summary points within the subsections of 10 CFR Part 73, Subpart E.

10 CFR Part 73, Subpart E	*Physical Protection Requirements of Special Nuclear Material and Spent Nuclear Fuel in Transit*
§73.24	Prohibitions
§73.25	Performance capabilities for physical protection of strategic special nuclear material in transit
§73.26	Transportation physical protection systems, subsystems, components, and procedures
§73.27	Notification requirements
§73.28	Security background checks for secure transfer of nuclear materials
§71.35	Requirements for physical protection of irradiated reactor fuel (100 grams or less) in transit
§73.37	Requirements for physical protection of irradiated reactor fuel in transit
§73.38	Personnel access authorization requirements for irradiated reactor fuel in transit

10 CFR Part 20 contains standards for radiation exposures of workers and the public. These regulations could be relevant when transporting a microreactor containing its unirradiated or irradiated nuclear fuel (10 CFR Part 20).

Other requirements relevant to microreactor transport would be standards outlined by the American Society of Mechanical Engineers (ASME). These standards are highlighted because it will be important to assess the quality and structural integrity of the reactor's components, both before and after transportation. The relevant ASME sections would depend on reactor design, but a relevant section for general standards would be the ASME Boiler and Pressure Vessel Code (BPVC), Section III, which governs the design, materials, fabrication, examination, testing, and certification of nuclear facility pressure boundary components, containment vessels, and supports (ASME 2025) often used in advanced nuclear reactors.

For a non-fueled microreactor with no radioactive material being transported, the regulation requirements would depend on the transport mode and required packaging of the reactor.

2.1 State Regulations and Policies

In the context of microreactor transport, the primary responsibilities of each state in the U.S. would be to issue overweight/over-dimension heavy-haul truck permits and to establish state preferred routes for radioactive material shipments based on 49 CFR Part 397. Each state could also choose to inspect highway microreactor shipments; however, these inspections would have to be coordinated among each state to avoid delays.

3.0 Shock and Vibration Physics Background

The following section highlights the relevant physics and dynamic behavior associated with periodic forces acting on a system. Understanding the forces that generate shock and vibration is important; however, it is equally important to characterize the system's dynamic response. The system response during transportation will determine the magnitude of the loads and vibrations experienced by the microreactor and, consequently, any potential damage that could later affect the safety and operation of the microreactor.

Vibration can be described as oscillatory motion of an object or system about an equilibrium position, caused by a time-varying force or motion. The response may be periodic or random movement. For a periodic response, the object's motion can be mathematically described using sinusoidal functions. The sinusoidal function has an amplitude, which describes the magnitude of the oscillatory movement, and a frequency that defines the number of cycles of oscillatory movement completed per second, in units of hertz (Hz) (SVANTEK n.d.). An object, or system of objects, has unique characteristics that influence the resonance frequency. The resonance frequency is the frequency that generates the maximum amplitude response. Specifically, if the forcing function acting on the system matches the resonance frequency, then the system absorbs energy and exhibits large-amplitude oscillatory motion. While vibration typically occurs over a long-duration time frame, a shock event occurs when a transient, high force acts on a system and causes large accelerations within the system over a transient time frame. Power spectral density (PSD) is a measure of the energy generated from vibrations at different frequencies.

The principles of vibration are directly applicable to the transportation of microreactors because the microreactor and its transport system can experience oscillatory excitation resulting from various external forces, including those generated by road conditions, the transportation mode, and the components used to secure and support the reactor.

Mathematically, an object's oscillatory responses to a periodic external forcing function over time *F(t)* can be defined for multiple degrees of freedom in the *x*, *y*, and *z* coordinate space. The response of the object is like the behavior of a simple spring or harmonic oscillator, whose acceleration vector ($\ddot{x}$), velocity vector ($\dot{x}$), and position (x) from a center or point of equilibrium can be modeled using a second order ordinary differential equation (ODE):

$$m\ddot{x} + c\dot{x} + kx = F(t)$$

where *m* is the mass of an object, *c* is the damping coefficient, and *k* is the stiffness coefficient. For a system of objects, the model becomes more complex because the oscillatory motion across the system could be interconnected and influence neighboring objects' behavior. The oscillatory behavior can still be mathematically represented, becoming a second-order, linear, matrix-valued ODE:

$$M\ddot{x} + C\dot{x} + Kx = F(t)$$

where *M* is the mass matrix that accounts for all the masses in the system, *C* is the damping matrix with all damping coefficients, and *K* is the stiffness matrix with all stiffness coefficients (Fan et al. 2026). This matrix-valued ODE can mathematically represent oscillatory motion within a system and be used to solve for the natural frequencies, as well as the magnitude of response from different time-varying forces.

4.0 Relevant Transportation Literature Background

The following section identifies relevant variables that will impact the road transportation of a microreactor. Limited studies and literature are currently available on the shock and vibration environments experienced by microreactors during road transportation. However, existing studies on heavy-duty truck transportation and nuclear fuel cask transportation can provide relevant insights. Although these studies do not provide direct representations of microreactor transport environments, they can be used as a proxy for microreactor shock and vibration analyses.

It should be noted that this section highlights the impact of variables to the overall transport system and does not distinguish the frequency responses for the vehicle, suspension, or microreactor/package individually. Different system components can have responses in different frequency ranges. Future analysis would be needed to determine these delineations and identify how external forces impact the magnitude of certain responses for parts within the transportation system (Park et al. 2020).

4.1 Road Quality and Vibration Energy

One of the major factors to consider for microreactor transportation via roads is the condition and type of road. The quality of the road surface can cause varying degrees of vibration and influence the frequency responses of both the vehicle and microreactor being transported. Road quality can include variables such as roughness or existing cracks. The type of road, defined in this report as the type of road material (STONECO 2024) could include asphalt, cement concrete, or chip seal used to resurface rural roads or gravel backroads.

Additionally, other road characteristics such as potholes, speed bumps, railroad tracks, could produce shock events. A study done by Foley and Gens (1968) analyzed the shock and vibration inputs during the transport of a radioactive materials cask transported by both railroad and truck. Of the 17 different road events they characterized during transport via truck—including unpaved roads, hills, overpasses, bumps, bridges, and more—the bumps and potholes produced the most severe responses for the cargo system (Foley and Gens 1968). The study reported that for a cargo system with natural frequencies above 15 Hz, crossing railroad tracks had a higher probability of causing more damage as compared to systems with lower natural frequencies. A study by Ranathunga et al. (2010) found that both poor and fair quality roads generated higher PSD levels, larger root mean square acceleration, and more shock events; also, this study highlighted how vehicle speed can be a co-dependent variable with road quality, which will be discussed in the next section.

To better understand the frequency response of a microreactor transport system impacted by road quality, it will be important to define a “normal terrain” of the road and record the frequency response when there are limited variables that produce large excitations or shocks to the system. This would serve as a baseline comparison to other aspects that might cause larger shock events in the future such as cracks, potholes, and bumps/drops. Further details regarding the methods to quantify road terrain quality will be provided in **Section 5.1.1**.

4.2 Vehicle Speed

Another variable that can impact the vibrations experienced during road transport is the vehicle speed. As mentioned above, vehicle speed and road quality might not always be independent

variables. A study by Lamb and Rouillard (2021) found that the level of vibrations for a road vehicle is a function of vehicle type (dynamic characteristics), road roughness, and vehicle speed. The previously mentioned study by Ranathunga et al. (2010) found high PSD levels for scenarios with higher vehicle speed on better road quality (defined as “fair”), as well as a lower vehicle speed on much lower quality roads (defined as “poor”). This highlighted that vehicle speed can contribute to more severe vibration responses, even when road conditions are relatively good. Another study of truck transport in Korea found that the vibration levels increased as the vehicle travel speed increased (Park et al. 2020). Future microreactor transport experiments should be intentionally designed to study the coupled effects of speed and road quality. These experiments could help determine the threshold speeds and road conditions that cause highly energetic frequency responses. Establishing these thresholds could help create mitigation strategies to avoid any damage or unanticipated loads to the microreactor system during transport.

4.3 Vehicle Suspension Type

Transporting a microreactor on road will most likely require a heavy-duty vehicle such as a truck with suspension that can carry weightier loads. Common suspension types for these commercial vehicles include leaf-spring and air-ride suspension systems (Lamb and Rouillard 2021). Suspension can impact the frequency range(s) and magnitude of acceleration that is imparted to the system from shock events and vibration. A study by Pierce et al. (1992) found that the levels of vibration recorded were around 50 percent higher for leaf-spring suspension, as compared to air-ride suspension trailers (Pierce et al. 1992). While this outcome is meant to highlight the impact of vehicle suspension on the system, it should not be applied as a general rule. The vibration experienced by a system will also depend on factors related to the payload itself. Future experiments regarding microreactor transport should incorporate early investigation into the appropriate vehicle suspension type for the specific microreactor being transported.

4.4 Payload and System Dynamics

Any system will have a natural frequency response (“resonant frequency”) like the harmonic oscillator system described in **Section 3.0**. The resonant frequency is the frequency that generates the maximum amplitude response of a particular object or system.

A time-varying force like vibration from road transport will affect the system differently depending on its resonant frequency. The microreactor being transported can be thought of as a spring-mass system because it will also exhibit oscillatory responses because of the external forces acting on it (from the vibrations of the road). A spring will have a certain stiffness and the spring-mass interconnection will have a damping factor. Both variables influence the dynamic response of the system to external forces. A spring’s stiffness affects the system’s natural frequency (for an undamped system), while damping will reduce the magnitude and width of that resonant response; for large enough damping it can also affect the natural frequency at which peak response occurs.

Quantifying these spring-mass system characteristics for the specific microreactor transport system will be important because they will impact the resonant frequency of the system and, therefore, the magnitude at which certain vibration frequencies will impact the system.

4.4.1 Payload Stiffness

A lower structural stiffness indicates a reduced ability to resist deformation. For a simple undamped spring-mass system with a given mass (*m*), the natural response period (T_n) is proportional to the square root of the spring stiffness (*k*) over the mass (*m*):

$$T_n \propto \sqrt{\frac{k}{m}}$$

$$f_n = \frac{1}{T_n}$$

For a given mass, if the spring stiffness (*k*) is larger, this results in a longer (or larger) natural response period (T_n). And since the natural period (T_n) is equal to the inverse of the natural frequency (f_n), a lower stiffness results in a reduced natural frequency (Fan et al. 2026). This could mean that for a less stiff microreactor transportation system, it is possible the system might have a larger dynamic response for lower-frequency excitations; if a system has a lowered resonance frequency, a lower-frequency input will produce maximum amplitude response. However, transportation of a microreactor and truck will not be a simple spring-mass system but rather a complex and interconnected system of springs, masses, and additional damping factors. Further modeling and analysis would be needed to determine the expected dynamic response and natural frequencies in the entire system. For future experiments, it will be important to note any contributions to system stiffness.

As mentioned above, a spring-mass system is influenced by three variables—mass, stiffness, and damping characteristics. While mass and stiffness primarily determine the system's natural frequencies, damping influences the magnitude of the resonant response, often reducing the amplitude of vibration near resonance. Analysis of the PSD from experimental data can show how road-induced vibration is distributed across different frequencies and how that translates into acceleration or displacement of the microreactor transport system. Comparing these experimental results with a matrix-based harmonic oscillator model that incorporates multiple mass, stiffness, and damping components could help to quantify the magnitude and location of damping contributions.

4.4.2 Payload Position and Axes of Acceleration

Another variable to consider for transporting a microreactor via road is the location of the microreactor within the vehicle. It has been reported in literature that the most severe location for vertical acceleration is typically over the rear axles of a truck or trailer (Maheras et al. 2013; Park et al. 2020). Across most frequencies, the middle of the trailer was found to generally have the least severe response (Maheras et al. 2013). Future shipments of microreactors might be a fully constructed reactor, while others might be shipped in parts. Therefore, future shock and vibration experiments should intentionally evaluate which parts of the microreactor are more vulnerable to damage from shock and vibration, and measure data that can help to quantify how position influences the magnitude of vibration transmitted to the particular microreactor system.

Additionally, different axes of vibration can result in different amplitudes of acceleration experienced by the system. It has been reported in numerous studies related to truck transportation that vertical vibration amplitudes are larger than lateral and longitudinal vibration amplitudes (Park et al. 2020; Foley and Gens 1968). One study by Pujet and Malesys (1989)

measured the vibration environment during truck transport of spent fuel transport casks, with a cask weighing around 36 metric tons, over a distance around ~1,600 km. Their reported acceleration values for truck transport mode in the longitudinal, transverse, and vertical axes were 1.8 g, 1.8 g, and 2.2 g, respectively. However, another study done by Prulhiere and Israel (1980) regarding the transport of radioactive fuel elements for a PWR reactor, reported accelerations measured on an assembly inside a used nuclear fuel cask (~110 tons). For the truck transportation mode, the longitudinal, traverse, and vertical accelerations were 0.15 g, 0.5 g, and 0.4 g, respectively. These studies show how the vertical axis can typically experience large accelerations; however, the Prulhiere et al. study also demonstrates how other axes like the transverse axis can additionally experience higher accelerations. For this reason, all axes of vibration should be monitored and assessed in future shock and vibration experiments for microreactor transportation.

There is a wider variety of available literature[2] on the transportation of nuclear fuel casks and other radioactive material, compared to microreactor transportation. While the studies reviewed in this report were not conducted specifically for microreactors, they demonstrate that measured acceleration responses can vary substantially depending on the characteristics of the transported system. Many currently proposed microreactor designs would be smaller and lighter than typical spent fuel shipments mentioned in this report. However, the literature review of nuclear fuel casks highlighted some of the characteristics that could impact measured acceleration of microreactor transport and should be considered, including the impact of the overall system's mass on the magnitude of measurement (for similar transport-type studies), the measurement location in the system, and the axis of acceleration measurement. These factors can produce significantly different acceleration responses even under similar transportation conditions.

For this reason, future microreactor transportation experiments should include preliminary testing and system calibration to characterize the unique dynamic response of the transportation system and establish representative baseline measurements. These baselines can then be used to compare responses across different road conditions, routes, and transportation configurations. Additionally, axes of measurement and reference points should be clearly defined before data collection.

4.4.3 Ranges of Frequency Response

Different frequency ranges produced by road vibration can correspond to different acceleration amplitudes. In a study done by Sandia National Laboratories, researchers measured shock and vibration inputs for the truck transport of a 15-ton, radioactive materials cask over 300 miles (Magnuson and Wilson 1977). Across the entire frequency range measured, 0–1,900 Hz, they found that the highest acceleration amplitudes (shock-like events) occurred in lower frequency ranges, 0–10 Hz, for longitudinal, traverse, and vertical axes. Additionally, it was found that in different frequency bands, the axis with the highest recorded acceleration could change.

Initial measurements will be required in the future to ascertain the relevant frequency ranges for the transportation system. Relevant frequencies of the external forces acting on the system could be impacted by variables such based on road roughness, truck speed, system stiffness, suspension types, and the system axis the force is acting upon.

[2] A literature review done by Maheras et al. (2013) provides more examples of truck transported nuclear fuel casks and ranges of measured acceleration.

4.4.4 Extreme Shock Events

The purpose of this study is to highlight variables relevant for the vibrations that may be experienced during road transport. Additionally, there has been mention of contributing factors for minor shock events, which are defined in this study as those that are commonly experienced by normal road travel (e.g., bumps, potholes, railroad tracks). However, it should be noted that there can be a possibility of larger shock events such as a vehicle crash. While these types of events are outside of the scope of this study, they will be an important area to study in the future to support safe and reliable transportation and deployment of microreactors. Alzahrani et al. (2025) develops an assessment methodology for how probable accidents might occur when transporting microreactors via road, rail, or maritime transportation modes. It also highlights associated consequences like radiological exposure, which would be relevant if a microreactor is transported with nuclear material or spent fuel.

5.0 Shock and Vibration Analysis

The following section will highlight how some of the previously identified variables, important to consider for microreactor transport, could be more clearly defined and measured for a hypothetical experiment using the road transportation mode.

5.1 Transportation Route Considerations

The transport route is a critical variable in shock and vibration testing because it will impact possible stressors on the transport system and the duration of the trip. Route selection in this report considers road quality, terrain and grade, and total distance/time duration of the trip. However, another factor that would be important to consider for a transport route is the population density and traffic congestion at certain locations—particularly when transporting a microreactor containing radioactive fuel.

Choosing a route considering these factors may involve trade-offs, depending on the objectives of the trip. For example, if the primary objective is to minimize vibration and shock severity, a route with the highest road quality rating may be preferred, as cracks or other surface irregularities can generate significant vibration-inducing inputs. Alternatively, if avoiding densely populated areas is a priority, secondary or back roads may offer advantages; however, these routes may also have poorer road conditions and therefore expose the microreactor to greater vibration levels. Also, if transport is time sensitive, using longer routes through back roads might require faster vehicle speeds to make up time and induce greater vibrational impacts. Or perhaps the objective is to minimize the total duration of exposure to shock and vibration; then, the most direct and efficient route may be more appropriate.

5.1.1 Road Roughness

Road quality was the first factor investigated for route optimization. Road quality can be measured as a longitudinal profile, which can include information regarding road grade, roughness, and texture (Karamihas and Sayers 2025). A longitudinal profile is often measured using a reference elevation, height relative to the reference, and the longitudinal distance over which the measurement is taken. There are specific procedures for measuring road profiles, depending on the length of the section and resolution required. Equipment that has been utilized for roughness measurements includes rod and level surveys, dipstick profilers, profilographs, or profiling devices[3] (Pavement Interactive n.d.; Karamihas and Sayers 2025).

One metric for road quality is the Present Serviceability Rating (PSR), but PSR is a subjective unit of measurement based on an individual's observations or "the judgment of an observer as to the current ability of a pavement to serve the traffic it is meant to serve" (Highway Research Board 1972). The International Roughness Index (IRI), defined by the Federal Highway Administration (FHWA), DOT (FHWA 2022), is the more common road roughness metric because it can be standardized in comparison to PSR. Road conditions across the United States are often classified using the IRI metric.

Modern IRI measurement methods use a laser height sensor to record the distance between the vehicle and road surface, an accelerometer to measure the vehicle's vertical acceleration,

[3] Further detail for the various roughness measurement approaches can be found in *The Little Book of Profiling*, Second Edition, https://deepblue.lib.umich.edu/items/11f2c531-1e70-4ffb-8058-5c4efb6b79ce.

and an instrument to track the total displacement of the vehicle. These measurements are combined to reconstruct the longitudinal profile of the road. The resulting profile is then used as the input to a standardized quarter-car model (**Figure 1**), which simulates the vehicle's response to the road profile and calculates the IRI based on the resulting relative suspension motion (FHWA n.d.).

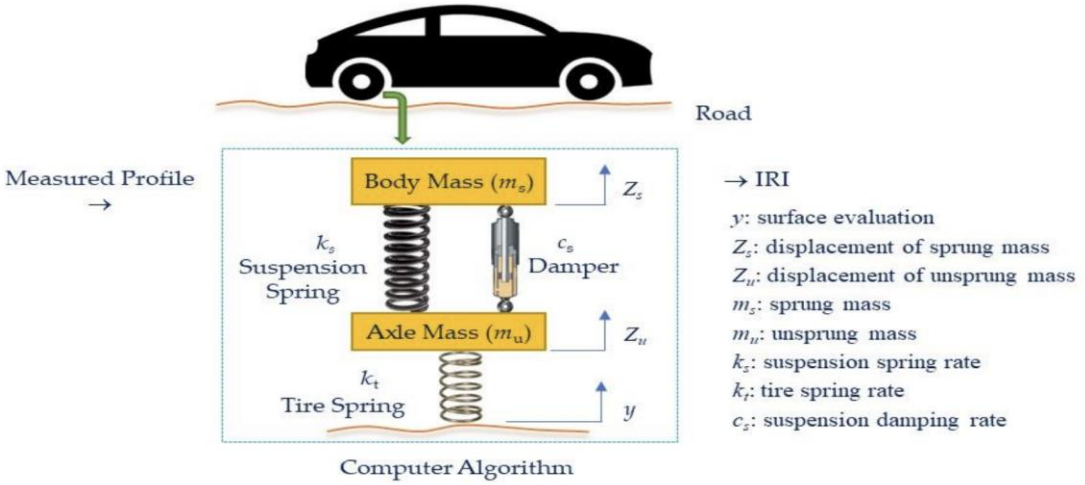


Figure 1. Diagram of the quarter-car model, showing IRI as a function of the surface evaluation (y, measured by in-situ road surveys) and the mass displacement (Z_s, Z_u) of a dual-spring system (with spring constants k_t, k_s) (Lin et al. 2022).

The units of IRI are typically meters per kilometer or inches per mile—a measure of accumulated displacement of a standard quarter-car model divided by the distance traveled. IRI data is collected along both major and secondary roadways across the U.S. and submitted annually by states to the FHWA through the Highway Performance Monitoring System (HPMS). HPMS makes this information publicly available and provides categorization thresholds to delineate between "good," "fair," and "poor" road quality (FHWA 2026). The distribution of IRI for the national highway network and the states is shown in **Figure 2** below.

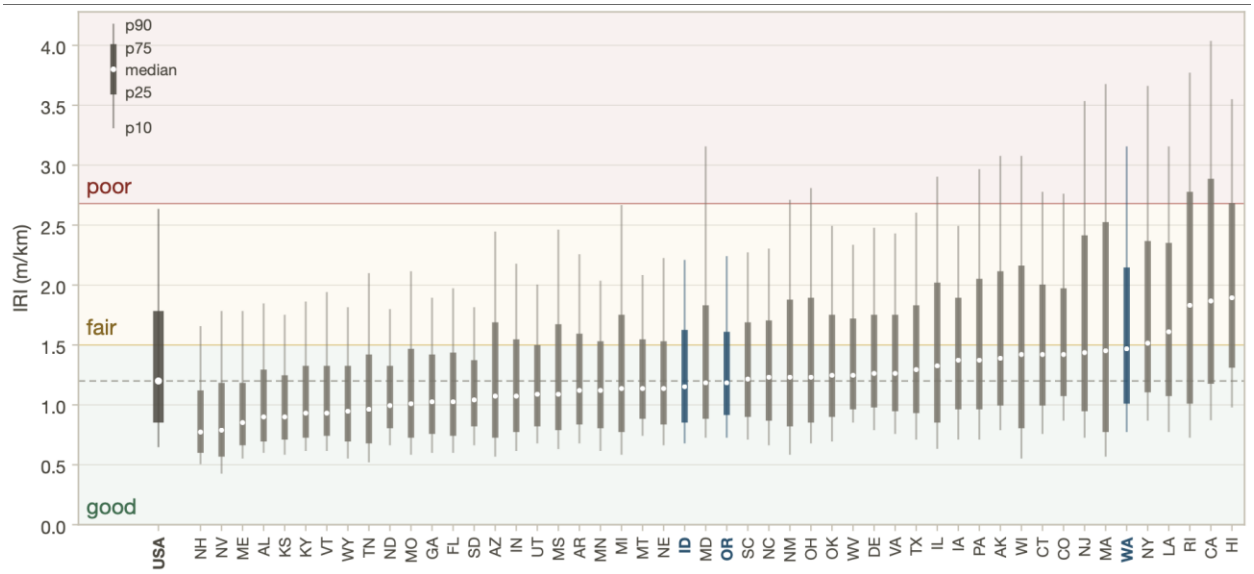


Figure 2. Distribution of IRI for the national highway network across the U.S. and individual states (FHWA 2026). Each state boxplot has a representative range, including the median IRI rank (white dot), the interquartile range, and whiskers for the tenth and ninetieth percentiles of roads. Established IRI metrics from FHWA for poor (red), fair (yellow), and good (green) road conditions are defined as ≤ 1.50 m/km, between 1.50 and 2.68 m/km, and ≥ 2.68 m/km, respectively. These thresholds are overlaid on the graph as horizontal-colored regions.

5.1.2 START Route Optimization

As part of this study, a transportation and logistics algorithm was developed to optimize a few possible scenarios for a particular route that could be used to transport a microreactor via road, from the Idaho National Laboratory (INL) to the Port of Seattle. Several potential routes were identified for a microreactor being transported from the Port of Seattle to INL. Different routes were chosen based on different criteria or optimization objectives, including a Stakeholder Tool for Assessing Radioactive Transport, or START route, minimization of poor road quality exposure (lowest peak IRI), reducing overall travel time, and avoiding population centers. **Figure 3** shows the START-derived route alongside routes derived from other optimization functions.

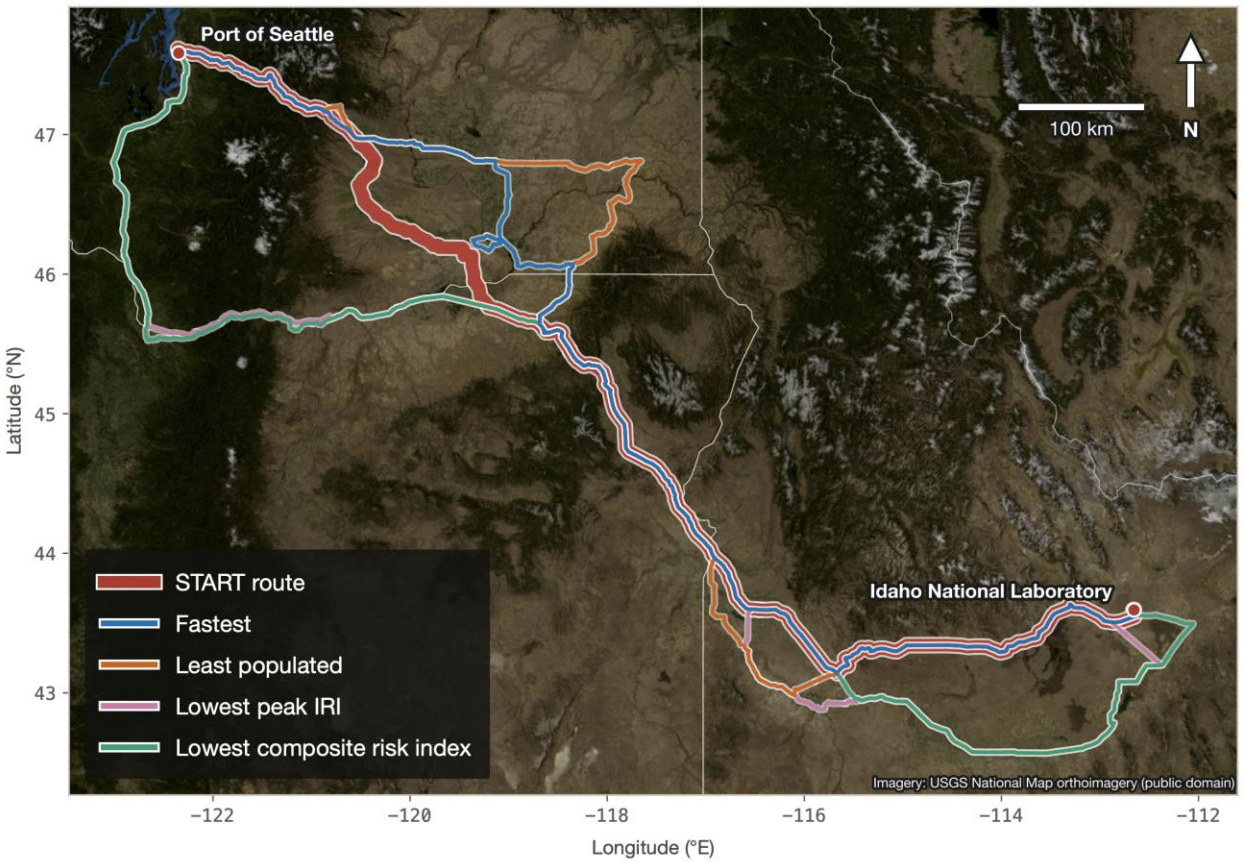


Figure 3. Representative results of a route optimization study for road transport between the Port of Seattle to INL. Different routes are shown based on different criteria or optimization objectives, including a START route, minimization of poor road quality exposure (lowest peak IRI), highest reduction of overall travel time (fastest), the route that reduces the transportation near populated areas, and the lowest composite risk index. The composite risk score was defined as an equal-weighted example considering IRI, curvature, grade, and population exposure and can be tuned to reflect priorities.

Additionally, combining other datasets (e.g., topography, population density, bridge load and clearance data, accident rate) allows for a detailed and flexible assessment of a route's risk profile ("Lowest composite risk index" route in **Figure 3**). A composite risk score can be easily developed from these metrics with customizable weights that reflect asset-specific needs and priorities. An example of this analysis is illustrated in **Figure 4**, showing IRI rating along with road and terrain classes, curvature, and grade for the START route between INL and the Port of Seattle.

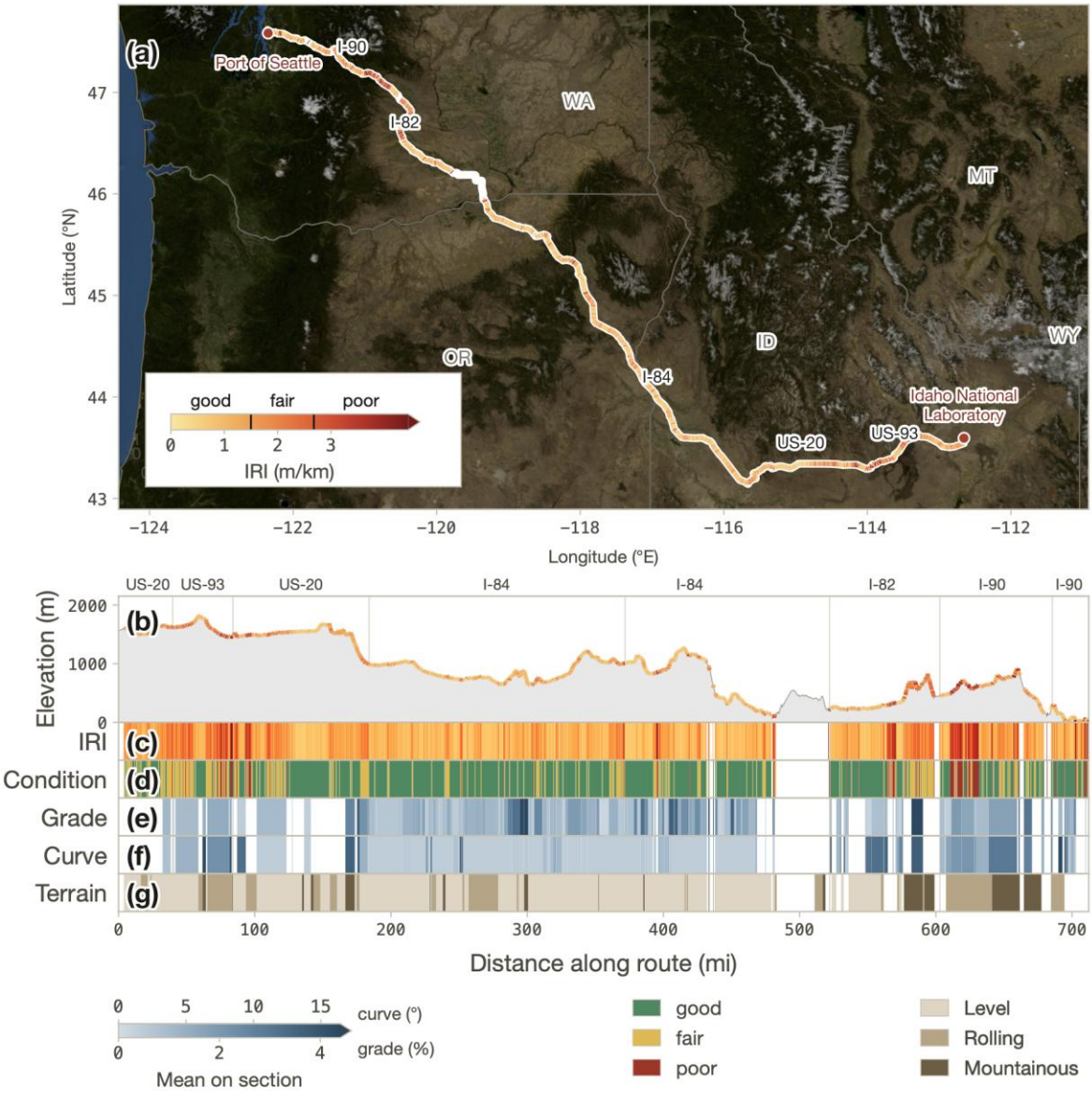


Figure 4. Resulting metrics from the developed transportation route selection algorithm, which utilize publicly available HPMS road quality data. These results are for a START route for microreactor transportation, highlighting the IRI rating, terrain classes, curvature, and grade for the entire route. Metrics are reported at different scales, normalized to 1 km segments. This analysis can be applied in the future to any transport route to inform optimized route decision-making.

The developed transportation route selection algorithm, which utilizes publicly available HPMS road quality data, was applied to a START route for microreactor transportation, and researchers produced the IRI rating, terrain classes, curvature, and grade for the entire route. This analysis can be applied in the future to any transport route to inform optimized route decision-making.

While this case study illustrates the potential for microreactor transport routes in the Pacific Northwest, this approach could be transferred to other sensitive transportation applications. The

utility of this route optimization algorithm depends on the integrity of the IRI data, which can be validated using test runs along these routes. Observational studies using accelerometers or other sensors would allow for an empirical mapping between IRI ratings and physical shock and vibration stress.

5.2 Accelerometers and Other Sensors

Accelerometer selection and placement are important considerations for a future microreactor shock and vibration experiment. Sensor type, measurement range, resolution, sampling rate, data storage capacity, battery life, and calibration should all be evaluated to ensure that the collected data adequately characterizes the transportation environment.

There are alternating-current accelerometers, with common types being “charge accelerometers” or “Integrated Electronics Piezo-Electric accelerometers;” alternatively, there are direct current (DC) accelerometers, including “capacitive,” “piezoresistive,” or “micro-electro mechanical system (MEMS)” sensors, which can be either capacitive or piezoresistive (Smith 2022). Piezoelectric accelerometers are commonly used for dynamic vibration measurements because of their broad frequency response (PCB n.d.).

The type of accelerometer can impact the noise in the output signal, the signal conditional requirements, device size, and the range of measurement and sensitivity. For example, for a variable capacitive MEMS accelerometer, the device has a lower range but higher sensitivity for acceleration measurements; alternatively, a piezoresistive MEMS accelerometer has a higher range of detection but lower sensitivity.

The selected sensor should have sufficient measurement range and resolution to capture both low-amplitude vibrations and higher-magnitude shock events without saturation. Initial tests and experimentation with devices might be required to ensure adequacy of the device. The sampling rate should be sufficiently high to capture all the characteristic responses for the duration of the transport. Depending on the duration of the shock and vibration experiment, a possible option for data collection could be a continuous sampling rate, though the sampling rate will also be dependent on the overall data storage capacity available in the sensor. Data storage capacity and battery life are factors that should be evaluated to make sure that adequate data collection will be possible for the entire duration of the transportation test. Calibration before testing must be done before any experiments to verify sensor sensitivity, frequency response, measurement range, and data acquisition performance.

Finally, future experiments should consider the number of axes that the accelerometer can record, and if multiple types of sensors may be needed. The most common accelerometer measures along a single axis; however, there are triaxial accelerometers that can record vibrations along the lateral, transverse, and rotational axes (Emerson n.d.).

Also, planning should be done to determine the placement of the sensors throughout the microreactor transportation system, which will provide the most thorough representation of the system response in transit. In a spring-mass system, large vibration responses occur near resonant frequencies and at locations that are more flexible or experience greater dynamic motion, such as beam midpoints, cantilever tips, or structural interfaces. Similarly, acceleration measurements can vary depending on the location on the microreactor (e.g., high, middle, and low positions) and at different locations within the truck bed. Therefore, preliminary testing and calibration should be used to identify appropriate sensor locations and verify that the selected

sensors can capture the relevant acceleration magnitudes and frequency range before conducting a full-scale transportation experiment.

The objectives and conditions of the shock and vibration experiment will determine which accelerometer sensor will be the best choice to adequately collect data. However, some initial accelerometer types are highlighted in **Table 4**, which could be utilized in a future experiment.

Table 4. List of different types of accelerometers that could be used for future shock and vibration experiments.

Sensor Type	Measurement Range (g)	Resolution	Frequency Response	Samples per Second	Battery Life; Operating Temp
GP-1 Accelerometer (SENSR n.d.)	+- 6.7 g	0.001 g	DC 50 Hz	100 sps	> 40 days (-4 to 176 degrees Fahrenheit)
High-Performance Accelerometer (Wilcoxon-797) (Wilcoxon n.d.[a])	80 g peak	100 mV/g (+- 5% sensitivity tolerance)	1–12,000 Hz (+- 3 dB)	Unknown	(-50 to 120 degrees Celsius)
Triaxial accelerometer (Wilcoxon 993A) (Wilcoxon n.d.[b])	50 g peak	100 mV/g (+- 10% sensitivity tolerance)	2–2,000 Hz frequency	Unknown	Unknown

Other sensors that could be relevant for shock and vibration analyses include a velocity sensor to record the vehicle speed during transport or a strain gauge that can measure structural loading. A strain gauge could be useful if there are tie downs or structures used to secure the microreactor within the transport vehicle.

5.3 Microreactor Integrity Assessment

Depending on the reactor type being transported, there will be different materials used for internal and structural components. It is less likely for an ideal road transport scenario to cause complete failure of the material components in the microreactor, unless there is a major crash or impact event. However, the magnitude and duration of sustained loads to different materials could lead to degradation or amplify existing vulnerabilities within the material—both of which could compromise reactor function in the future.

For this reason, the development of a shock and vibration experiment should include the characterization of certain materials' integrity before and after transportation. External stimuli, such as vibration or major shock events, will impact certain materials differently and different materials or components may be particularly vulnerable, such as weldments or brittle ceramic materials. The successful transport of a microreactor must include identification and mitigation of any possible defects that could be caused by transportation-induced loads.

5.3.1 Considerations for Metallic Reactor Components

Many material components will be reactor-specific; however, common materials that have been utilized for advanced nuclear reactor designs include nickel-based superalloys or stainless steels (a specific example includes 316H austenitic stainless steel). These metal-alloys are utilized because of their high mechanical strength and resistance to corrosion. The higher concentrations of alloying elements, such as chromium in superalloys or stainless-steel alloys, can result in the formation of a semi-protective layer to protect the base alloy as the chromium selectively reacts with the surrounding high-temperature corrosive environment.[4] Advanced reactor designs that utilize liquid metals or molten salts could potentially utilize these metallic alloys for guard vessels, grid plates, and/or support and bearing plates. Literature reports that the 316H austenitic stainless steel has been utilized for structural components and piping systems for Generation IV nuclear reactor designs because of its resistance to extreme thermal stresses, which would be found in the corrosive environments created during operation (Xu et al. 2021; Dai et al. 2021; Xu et al. 2022).

However, despite the alloys' high strength and corrosion resistance, a possible vulnerability lies in the weld features between the metallic components of the reactor. While there are standards for welding and weld design, other variables can introduce defects or stresses within the weld. These variables could be incorrect process parameters, improper weld execution, or incompatibilities between materials or additional servicing that can cause unanticipated outcomes (Somers and Pense 1994). Welding can generate surface tensile stresses, but also other procedures can cause residual stresses throughout the material such as plastic deformation of the material during production, heating/cooling, or chemical surface treatments (Mgonja 2017). These residual stresses remain in the material after manufacture, and the magnitude of residual stresses can impact the integrity of the material. When internal stresses, like the residual stresses caused by production, exceed the strength of either the weld metal or base metal, there is a possibility for cracks to form. Depending on the magnitude of the crack defect, it can cause premature failure of the weld because of stress being concentrated at the crack site (Yousefi et al. 2015; Mgonja 2017). To avoid failure of the reactor materials during operation, it is important to identify any pre-existing residual stresses or vulnerabilities in the material that could be aggravated by vibration or shock events during transport. Typical techniques that can be used to identify any weld joint failure or defect include visual examination, optical microscopy, or an analytical study of stress on the material (Somers and Pense 1994).

For future analysis, material characterization before and after transport could be done on the welded joints of the microreactor or reactor proxy. Observation of the material and quantified vibrational impacts experienced during transportation could help to inform mitigation strategies for future microreactor deployment.

5.3.2 Considerations for Ceramic Reactor Components

Ceramic materials are also often used in advanced reactors because of their resistance to high temperatures, corrosive environments, and radiation effects. Ceramics have ionic and covalent bonds within their crystalline structures; ceramics are less resilient to accommodating applied stresses because of their strong, directional atomic bonding in the crystalline structure which restricts plastic deformation mechanisms. This differs from metals whose atomic bonding and

[4] Exact corrosion kinetics and thermodynamic pathways will depend on the temperature, pressure, and composition of the specific surrounding environment.

crystalline structure allows the redistribution and formation of dislocations to absorb the applied stresses without material failure. Ceramics typically undergo brittle fracture when a force exceeds the fracture strength or when there are pre-existing flaws or defects that act as stress concentration sites. Additionally, crystallographic orientation and microstructure can influence the ceramic material's susceptibility to crack initiation and propagation, potentially contributing to failure under applied loading.

The Antares-1 microreactor utilizes both graphite and a ceramic material, boron-carbide, for the control drums in the reactor (Antares n.d.). Another ceramic, Beryllium oxide, is commonly used in advanced nuclear reactors as a stationary core reflector system (Weber et al. 1957). Pre- and post-transportation characterization of the ceramic components' integrity will help mitigate amplification of any pre-existing defects that could lead to failure, as well as identify the threshold at which transportation can cause significant damage to ceramic materials because of any shock events. Techniques that could be utilized include visual inspection, optical, or electron microscopy, or ultrasonic instruments.

5.4 Functions and Requirements for Shock and Vibration Testing

A report published by Stewart et al. (2026) outlined a potential set of requirements and functions for a shock and vibration experiment for transporting a prototype reactor via roads. This set of requirements was created assuming the possible transport of a reactor within the microreactor application research validation and evaluation (MARVEL) program.

Table 5 highlights those defined requirements and these are included in this report because they could provide a useful framework for future experiments that seek to analyze the impacts of shock and vibration on a microreactor system being transported via roads. Requirements were included for both road transport experiments, as well as laboratory-based tests on a vibration table.

Some of the requirements were developed based on DOD/DOW test-method standard MIL-STD-810H, which consists of a series of minimum test conditions for military equipment and systems. Specifically, the MIL-STD-810, Method 514 (Department of Defense 2019a) and Method 516 (Department of Defense 2019b) were referenced because of their focus on vibration testing and shock testing, respectively.

Table 5. Functions and requirements for shock and vibration testing for MARVEL reactor shock and vibration study. Provided from the report by Stewart et al. (2026).

Req #	Requirement or Function
SV1	Equipment shall be loaded, packed, and secured in a manner consistent with field deployment (e.g., relatively compact packing in a minimum number of vehicles) (Department of Defense 2019a, Method 514.8, 4.1.3).
SV2	The testing route or routes should be chosen to provide as wide and representative a range of service conditions as possible (Department of Defense 2019a, Method 514.8, 4.1.3).
SV3	Total distance traveled during testing should approach distances that would likely be encountered during a field deployment of a microreactor (Department of Defense 2019a, Method 514.8, Annex C, 1.2). The approximate distance from the Mean Center of Population to coastal populations is 1,000 miles (U.S. Census Bureau 2021). A range given for military mission/field transportation is 300–500 miles (Department of Defense 2019a, Method 514.8, Annex C, 2.1.2).

Req #	Requirement or Function
SV4	Road speed during testing should cover a range typical for travel on U.S. highways, subject to safety requirements and local speed limits.
SV5	Where dunnage is used in place of system elements that could be present during transportation for field deployment (e.g., fuel assembly in reactor bore), it should be designed to resemble the mass, geometry, and harmonics of the corresponding system elements.
SV6	Where feasible, shock and vibration data should be obtained on individual reactor components, subassemblies, and structures.
SV7	Shock and vibration data shall be collected on structures used for crating and packaging of reactor components, subassemblies, and structures, especially in cases where it is not possible to collect data on the structures themselves.
SV8	Shock and vibration data shall be collected on conveyances used to transport significant reactor structure.
SV9	Vehicle travel paths shall be recorded using time-indexed GPS data.
SV10	Mass of accelerometer sensors attached to components shall be minimized where attached mass is expected to affect vibration behavior.
SV11	Accelerometers featuring wireless data transmission or on-board data acquisition and recording shall to be used where system geometry precludes the use of cables or leads between sensors and data acquisition equipment.
SV12	Accelerometers shall be securely attached according to manufacturer recommendations.
SV13	Shock and vibration shall be measured along every relevant axis at a given location.
SV14	Any laboratory testing of components using a vibration table shall utilize appropriate vibration exposure spectra for ground transportation over U.S. highways (e.g., Department of Defense 2019a, Method 514.8, Annex C, Figure 514.8C-2), ideally informed by representative field measurements.
SV15	Accelerometers attached directly to reactor systems or components shall be attached using methods and contact materials approved by the appropriate design authority to prevent damage and contamination.
SV16	Acceptance inspections of components and functional testing of subsystems, as applicable, shall be carried out before and after shock and vibration testing (Department of Defense 2019a, Method 514.8, 4.5.4, and Department of Defense 2019b, Method 516.8, 2.2.1).
SV17	Time-indexed ambient temperature shall be recorded along transportation routes during tests (Department of Defense 2019b, Method 516.8, 2.3).
SV18	Where feasible, time-indexed temperature shall be recorded during tests within enclosed structures or crates containing reactor components (Department of Defense 2019b, Method 516.8, 2.3).
SV19	Accelerometer transducers shall have a flat frequency response within ± 5% across the frequency range of interest (Department of Defense 2019a, Method 514.8, 4.2.3).
SV20	Accelerometer transducers shall have transverse sensitivity less than or equal to 5% (Department of Defense 2019a, Method 514.8, 4.2.3).
SV21	Temperature sensitivity deviations of accelerometer transducers at test temperatures shall be less than or equal to ±5% relative to the temperature at which the transducer sensitivity was established (Department of Defense 2019a, Method 514.8, 4.2.3).

6.0 Conclusion

The purpose of this report is to highlight important variables which are relevant for a microreactor being transported on a road, including regulatory requirements and system parameters. Additionally, general considerations and methodology were highlighted for a future transport experiment of a microreactor.

A companion document, *MARVEL Shock and Vibration Test Plan* (Peoples et al. 2026) establishes the procedures, functional objectives, and laboratory testing methodology for transportation shock and vibration qualification, building directly upon the functions and requirements developed in the *MARVEL Reactor Shock and Vibration Functions and Requirements Document* (Stewart et al. 2026).

The reactor type, as well as whether its fuel or radioactive materials are transported simultaneously, will influence the federal and state regulations applicable to the transport. A literature review of heavy-duty truck transport, or road transport of nuclear fuel in casks, was used as a proxy for microreactor transport to identify several variables that could impact the magnitude and frequency range of the system's response to vibrations from the road. These included road quality, vehicle speed, and vehicle suspension. Additionally, the review provided insights into potential behavior of the system based on factors like payload stiffness and position of the microreactor placement.

The transportation route was another key consideration for future microreactor deployment. A transportation algorithm was developed to identify potential routes that could be utilized in a future shock and vibration experiment, highlighting the trade-offs between road quality and time duration of travel. Selecting the route with the lowest IRI rating for road quality could establish a baseline where researchers could quantify how the road quality and the resulting vibrations affect the transport system. To further expand on the details required for this future work, sensor requirements, material integrity assessments, and functional requirements were outlined in later sections of this report.

The successful future deployment of microreactors in the U.S. will partially depend on the ability to characterize transportation-related impacts and mitigate any potential damage to the microreactors that could cause operational complications in the future. This work is intended to support the development of well-planned experiments to evaluate these effects.

7.0 References

10 CFR §§ 71.11–71.75. 2026. “Packaging and Transportation of Radioactive Material.” Electronic Code of Federal Regulations. Last updated August 26, 2026. Accessed August 2026 at https://www.ecfr.gov/current/title-10/chapter-I/part-71.

10 CFR §§ 73.24-73.38. 2026. “Subpart E, Physical Protection of Plants and Materials.” Electronic Code of Federal Regulations. Last updated August 26, 2026. Accessed August 2026 at https://www.ecfr.gov/current/title-10/chapter-I/part-73.

10 CFR Part 20. 2026. “Standards for Protection Against Radiation.” Electronic Code of Federal Regulations. Last updated August 26, 2026. Accessed August 2026 at https://www.ecfr.gov/current/title-10/chapter-I/part-20.

Alpha Tech. n.d. Website home page. Accessed July 2026 at https://alphatechresearchcorp.com/info/affordable-clean-energy.php.

Alzahrani, Y.A., M. Prins, T.M. O’Connell, A.S. Batikh, and M.A. Diaconeasa. 2025. “Integrated Probabilistic Risk Assessment Framework for Transporting Microreactors with a Case Study for Road, Rail, and Maritime Transportation Modes.” *NPJ Clean Energy* 1 (7). https://doi.org/10.1038/s44406-025-00007-3.

Antares. n.d. Website home page. Accessed August 2026 at https://antaresindustries.com/.

ASME. 2025. *BPVC Section III – Rules for Construction of Nuclear Facility Components, Subsection NCA, General Requirements for Division 1 and Division 2.* BPVC.III.NCA, American Society of Mechanical Engineers. Accessed August 2026 at https://www.asme.org/codes-standards/find-codes-standards/bpvc-section-iii-subsection-nca-general-requirements-div-1-div-2/2025/print-book.

CNSC. n.d. “Public Summary – Containment for Novel Reactor Designs.” Canadian Nuclear Safety Commission. Accessed August 2026 at https://www.cnsc-ccsn.gc.ca/eng/reactors/new-reactor-power-plant-projects/readiness-to-regulate-small-modular-reactors/four-pillars/containment/.

Dai, Y., X. Zheng, and P. Ding. 2021. “Review on Sodium Corrosion Evolution of Nuclear-Grade 316 Stainless Steel for Sodium-Cooled Fast Reactor Applications.” *Nuclear Engineering Technology* 53: 3474–3490. https://doi.org/10.1016/j.net.2021.05.021.

Department of Defense. 2019a. “Method 514.8—Vibration.” In *Environmental Engineering Considerations and Laboratory Tests* (MIL-STD-810H), 514.8-1–514.8-62. Washington, DC: Department of Defense.

Department of Defense. 2019b. “Method 516.8: Shock.” In *Environmental Engineering Considerations and Laboratory Tests* (MIL-STD-810H), 516.8-1–516.8-40. Washington, DC: Department of Defense.

Derr, E. 2022. “Nuclear Needs Small Amounts of Land to Deliver Big Amounts of Electricity.” Nuclear Energy Institute, Washington, DC. April 29, 2022. Accessed January 2026 at https://www.nei.org/news/2022/nuclear-brings-more-electricity-with-less-land.

Emerson. n.d. “Measuring Vibration with Accelerometers.” Sensor Fundamentals, Emerson. Accessed July 2026 at https://www.ni.com/en/shop/data-acquisition/sensor-fundamentals/measuring-vibration-with-accelerometers.html?utm.

Fan, T., H. Wu, C. Chen, X. Sun, and L. Wang. 2026. “Vibration Characteristics Analysis of Different Supporting Structures for Onboard Equipment of Lage-Scale Vehicles During Transportation.” *Progress in Nuclear Energy* 196: 106337. https://doi.org/10.1016/j.pnucene.2026.106337.

FHWA. 2022. “HPMS Field Manual, Appendix E: Measuring Pavement Roughness.” Federal Highway Administration, Department of Transportation. Last updated October 12, 2022. Accessed August 2026 at https://www.fhwa.dot.gov/ohim/hpmsmanl/appe.cfm.

FHWA. 2026. “LTPP InfoPave: Data Bucket.” Federal Highway Administration, Department of Transportation. Accessed August 2026 at https://infopave.fhwa.dot.gov/Databucket/Databucket.

FHWA. n.d. “Pavements – Inertial Profiler – Pavement (IP).” Federal Highway Administration, Department of Transportation. Accessed August 2026 at https://infotechnology.fhwa.dot.gov/inertial-profiler-road-pavement/?utm.

Foley, J.T., and M.B. Gens. 1968. *Shock and Vibration Measurements During Normal Rail and Truck Transport*. Report. U.S. Atomic Energy Commission 905-933. https://digital.library.unt.edu/ark:/67531/metadc1026805/m2/1/high_res_d/4701246.pdf.

GenIV. n.d. “Generation IV Goals, Technologies and GIF R&D Roadmap.” GenIV International Forum. Accessed July 2026 at https://prod2.gen-4.org/generation-iv-criteria-and-technologies?utm.

Highway Research Board. 1972. *National Cooperative Highway Research Program Synthesis of Highway Practice 14: Skid Resistance*. 1972. Highway Research Board, National Academy of Sciences, Washington, D.C.

HolosGen. n.d. “Technology.” Accessed July 2026 at https://www.holosgen.com/technology/.

Karamihas, S.M., and M.W. Sayers. 2025. *The Little Book of Profiling, Second Edition: Basic Information About Measuring and Interpreting Road Profiles*. The Regents of the University of Michigan. Accessed July 2026 at https://deepblue.lib.umich.edu/items/11f2c531-1e70-4ffb-8058-5c4efb6b79ce.

Lamb, M.J., and V. Rouillard. 2021. “On the Parameters that Influence Road Vehicles Vibration Levels.” *Packaging Technology and Science* 34 (9): 525–540. https://doi.org/10.1002/pts.2592.

Last Energy. n.d. “PWR-20: Engineered for Modular, Factory Production.” Accessed July 2026 at https://www.lastenergy.com/technology.

Li, C., S.L. Chen, C. Tang, and H.A. Hsieh. 2022. “A Study on the Roads Flatness Using International Roughness Index in New Taipei City.” *Journal of Physics: Conference Series* 2160: 012035. In 9th Annual International Conference on Material Science and Environmental Engineering (MSEE 2021), November 26–28, 2021, Nanjing, China. https://doi.org/10.1088/1742-6596/2160/1/012035.

Magnuson, C.F., and L.T. Wilson. 1977. *Shock and Vibration Environments for Large Shipping Containers on Rail Cars and Trucks.* SAND76-0427, Sandia National Laboratories, Albuquerque, New Mexico. https://www.osti.gov/servlets/purl/7305222.

Maheras, S.J., E.A. Lahti, and S.B. Ross. 2013. *Transportation Shock and Vibration Literature Review.* PNNL-22514, Pacific Northwest National Laboratory, Richland, Washington. https://www.osti.gov/servlets/purl/1083410.

Mgonja, C.T. 2017. "The Consequences of Cracks Formed on the Oil and Gas Pipelines Weld Joints." *International Journal of Engineering Trends and Technology* 54 (2): IJETT-V54P232. https://doi.org/10.14445/22315381/IJETT-V54P232.

Nuclear Engineering International. 2024. "HALEU UF6 and SMR Fuel Fabrication." June 20, 2024. Accessed July 2026 at https://www.neimagazine.com/analysis/haleu-uf6-and-smr-fuel-fabrication/.

NUSCALE. n.d. "SMRS vs Microreactors: What's the Difference?" NUSCALE POWER. Accessed July 2026 at https://www.nuscalepower.com/exploring-smrs/smr-101/smrs-vs-microreactors-whats-the-difference.

Office of Nuclear Energy. n.d. "Benefits of Small Modular Reactors (SMRs)." Department of Energy, Office of Nuclear Energy. Accessed August 2026 at https://www.energy.gov/ne/benefits-small-modular-reactors-smrs.

Park, J., S. Choi, and H.M. Jung. 2020. "Measurement and Analysis of Vibration Levels for Truck Transport Environment in Korea." *Applied Sciences* 10 (19): 6754. https://doi.org/10.3390/app10196754.

Pavement Interactive. n.d. "Pavement Evaluation: Roughness." Accessed August 2026 at https://pavementinteractive.org/reference-desk/pavement-management/pavement-evaluation/roughness/.

PCB Piezotronics. n.d. "Introduction to ICP Accelerometers." Accessed August 2026 at https://www.pcb.com/resources/technical-information/introduction-to-accelerometers.

Peoples, V., J. Sahagun, M. Stewart, J. Whitley, and S. Maheras. 2026. *MARVEL Shock and Vibration Test Plan*. INL/RPT-26-95163. Idaho National Laboratory, Idaho Falls, Idaho.

Pierce, C.D., S.P. Singh, and G. Burgess. 1992. "A Comparison of Leaf-Spring with Aircushion Trailer Suspensions in the Transport Environment." *Packing Technology and Science* 5 (1): 11–15. https://doi.org/10.1002/pts.2770050104.

Prulhiere, J.P., and F. Israel. 1980. "Measurement of Vibrational Effects on an Assembly of PWR Fuel Elements During Handling and Transport By Road and Rail." In Proceedings of 6th International Symposium on the Packaging and Transportation of Radioactive Materials, 1292–1301. November 10–14, 1980, Berlin, West Germany.

Pujet, D., and P. Malesys. 1989. "Measurement of the Acceleration Undergone by the Trunnions of Irradiated Fuel Transport Flasks During Normal Use." In Proceedings of 9th International Symposium on the Packaging and Transportation of Radioactive Materials, 932–939. June 11–16, 1989, Washington, D.C.

Ranathunga, C.L., H.H.E. Jayaweera, S.K.K. Suraweera, S.C. Wattage, K.K.D.L. Ruvinda, and T.R. Ariyaratne. 2010. “Vibration Effects in Vehicular Road Transportation.” Proceedings of the Technical Sessions 26: 9–16. Institute of Physics, Sri Lanka. https://ipsl.lk/documents/TechSession/2010/ipsl10-02.pdf.

SENSR. n.d. “GP1-L Recording Accelerometer.” SENSR, Structural Monitoring Solutions. Accessed August 2026 at https://www.sensraccelerometers.com/.

Smith, G.M. 2022. “Measuring Shock and Vibration with Accelerometer Sensors.” DEWESoft. January 5, 2022. Accessed August 2026 at https://dewesoft.com/blog/measure-shock-vibration-with-accelerometers.

Somers, B.R., and A.W. Pense. 1994. “Welding Failure Analysis.” *Materials Characterization* 33 (3): 295–309. https://doi.org/10.1016/1044-5803(94)90049-3/.

Stauff, N., C.H. Lee, and C. Filippone. 2022. *Core Design of the Holos-Quad Microreactor.* ANL/NSE-22/4, Argonne National Laboratory, Chicago, Illinois. https://doi.org/10.2172/1863405.

Stewart, M.L., V.O. Peoples, S.J. Maheras, and H.E. Adkins, Jr. 2026. *Functions and Requirements for MARVEL Reactor Shock and Vibration Study.* PNNL-39381, Pacific Northwest National Laboratory, Richland, Washington.

STONECO. 2024. “Choosing the Best Road Construction Materials.” December 2, 2024. Accessed July 2026 at https://www.stoneco.net/about-us/press/road-construction-materials.

SVANTEK. n.d. “Vibration Guide: Definition, Types, and Testing.” SVANTEK. Accessed July 2026 at https://svantek.com/academy/vibration-guide/.

Tarakanov, V. 2023. “What Is Uranium?” International Atomic Energy Agency. August 16, 2023. Accessed July 2026 at https://www.iaea.org/newscenter/news/what-is-uranium.

U.S. Census Bureau. 2021. “Centers of Population for the United States: 1950–2020.” U.S. Department of Commerce. Accessed March 2026 at census.gov.

Weber, W.P.; J.F. Quirk; A.W. Lemmon, Jr.; and R.B. Filbert, Jr. 1957. *Properties of Beryllium Oxide and Carbides of Beryllium, Molybdenum, Niobium, Tantalum, and Titanium*. Report No. BMI-1165, Metallurgy and Ceramics (TID-4500, 12th Ed.). https://www.osti.gov/servlets/purl/4379040.

Wilcoxon. n.d.(a). “High Performance General Purpose Accelerometer, 100 mV/g.” Wilcoxon Sensing Technologies. Accessed August 2026 at https://wilcoxon.com/premium-accelerometer-side-exit/.

Wilcoxon. n.d.(b). “3-axis Accelerometer with 4-pin Bendix Connector, 100 mV/g.” Wilcoxon Sensing Technologies. Accessed August 2026 at https://wilcoxon.com/993a/.

World Nuclear Association. 2025. “Nuclear Power Reactors: Molten Salt Reactors.” Last updated November 21, 2025. Accessed July 2026 at https://world-nuclear.org/information-library/nuclear-power-reactors/other/molten-salt-reactors.

World Nuclear Association. 2026a. “Current and Future Generation: Outline History of Nuclear Energy.” Last updated March 15, 2026. Accessed July 2026 at https://world-nuclear.org/information-library/current-and-future-generation/outline-history-of-nuclear-energy.

World Nuclear Association. 2026b. “Current and Future Generation: Fast Neutron Reactors.” Last updated March 31, 2026. Accessed July 2026 at https://world-nuclear.org/information-library/current-and-future-generation/fast-neutron-reactors.

World Nuclear Association. n.d. “Nuclear Essentials: Are There Different Types of Nuclear Reactor?” Accessed July 2026 at https://world-nuclear.org/nuclear-essentials/are-there-different-types-of-reactor.

Xu, L., C. Li, L. Zhao, Y. Han, and K. Hao. 2022. “Investigation on the Creep-Fatigue Crack Growth Behavior of 316H Welded Joints in Sodium-Cooled Fast Reactors.” *Engineering Failure Analysis* 141: 106684. https://doi.org/10.1016/j.engfailanal.2022.106684.

Xu, L., F. Bao, L. Zhao, Y. Han, H. Jing, and X. Gong. 2021. “Characterizing Microstructural Evolution and Low Cycle Fatigue Behavior of 316H Austenitic Steel at High-Temperatures.” *Journal of Nuclear Materials* 546: 152758. https://doi.org/10.1016/j.jnucmat.2020.152758.

Yousefi, M., M.H. Farghadin, and A. Farzadi. 2015. “Investigate the Causes of Cracks in Welded 310 Stainless Steel Used in the Flare Tip.” *Engineering Failure Analysis* 53: 138–147. https://doi.org/10.1016/j.engfailanal.2015.04.002.

Pacific Northwest National Laboratory

902 Battelle Boulevard
P.O. Box 999
Richland, WA 99354

1-888-375-PNNL (7665)

www.pnnl.gov